ELSEVIER

Process Biochemistry 34 (1999) 213–219

PROCESS BIOCHEMISTRY

Evaluation of methanogenic kinetics in an anaerobic fluidized bed reactor (AFBR)

V. Diez [a,*], P. A. García [b], F. Fdz-Polanco [b]

[a] *Department of Biotechnology and Food Science. University of Burgos, Plaza Misael Bañuelos s/n, 09001 Burgos, Spain*
[b] *Environmental Biotechnology Group, Department of Chemical Engineering, University of Valladolid, Prado de la Magdalena s/n. 47011 Valladolid, Spain*

Received 17 November 1997; received in revised form 16 February 1998; accepted 3 April 1998

Abstract

A kinetic study of the methanogenic phase was carried out on a pilot lab scale anaerobic fluidized bed reactor (AFBR) in batch mode. An examination of the effect of initial acetate concentration, bed expansion and bed segregation is presented.

Experimental data observed for the acetate removal against time were adjusted to a zero-order kinetic equation, over the chemical oxygen demand (COD) range studied (1430–5340 mg litre^{-1}), independently of the bed expansion (11–37%). The kinetic constant was calculated using robust regression analysis. The zero-order kinetic constant, K_0 was between 1180–1380 mg COD litre^{-1} h^{-1} on the fixed bed volume basis, and the maximum specific substrate utilization rate, k, was between 145–198 mg COD g VS^{-1} h^{-1}.

The kinetic behaviour was found to be different throughout the reactor, on the fixed bed volume basis and the activity at the bottom of the bed was lower than the activity in the upper region. However, on an attached volatile solids basis, the activity at the bottom level was the greatest.

Keywords: Wastewater; Anaerobic digestion; Fluidized bed; Kinetics; Mass transfer; Segregation

Nomenclature

Fundamental quantities

L	length
M_s	mass of substrate
M_x	mass of bacteria
T	time

Symbols

d_p	particle diameter
D_f	molecular diffusivity of substrate within the biofilm ($L^2\ T^{-1}$)
H	bed height
J	substrate flux ($M_s\ L^{-2}\ T^{-1}$)
k	maximum specific rate of substrate utilisation ($M_s\ M_x^{-1}\ T^{-1}$)
K_m	mass transport coefficient ($L\ T^{-1}$)
K_s	half-velocity coefficient ($M_s\ L^{-3}$)
K_0	zero-order kinetic constant ($M_s\ L^{-3}\ T^{-1}$)
K_{0i}	value determined at the ith run
S	concentration of rate-limiting substrate in the bulk liquid ($M_s\ L^{-3}$)
S_0	initial substrate concentration ($M_s\ L^{-3}$)
S_{0I}	initial substrate concentration at the ith run ($M_s\ L^{-3}$)
S_f	substrate concentration within the biofilm ($M_s\ L^{-3}$)
S_s	substrate concentration at the biofilm surface ($M_s\ L^{-3}$)
t	time (T)
V	water volume (L^3)
V_0	bed volume at minimum fluidizing conditions (L^3)
X	viable microbial concentration ($M_x\ L^{-3}$)
z	distance to the biofilm surface (L)

* Corresponding author.

0032-9592/99/$ - see front matter
PII: S0032-9592(98)00065-X

Greek symbols

ε_0 bed porosity at minimum fluidizing conditions
λ support biocovered surface fraction

1. Introduction

The advantages of anaerobic processes over aerobic processes have led to the development of different configurations of anaerobic processes capable of treating different types of wastewater. Fluidized bed technology can offer many advantages related to the use of small particles of support material for the accumulation of anaerobic bacteria, and the recirculation required to obtain sufficient upflow velocity which improves system mixing conditions and mass transfer.

The mathematical description of the fluidized bed bioreactor is relatively complex [1], basically for two reasons. Firstly, hydrodynamic characterisation is difficult, particularly in those systems where three phases are involved [2]. Secondly, the kinetic description must take into account all the phenomena taking place in the bioparticles, such as molecular diffusion, substrate consumption, product formation and cell growth.

In the anaerobic digestion of non-complex substrates, acetate conversion to methane and carbon dioxide is often accepted as rate-limiting [3]. This is due to the fact that the bacteria which ferment acetate to biogas produce about 70% of the methane and grow very slowly [4].

Mechanistically, substate removal may be described as the net result of the following steps:

1. Transport of material from the bulk fluid to the biofilm surface, or external mass transport, in which the substrate flux per biofilm surface area unit, J, is proportional to the substrate concentration gradient across the liquid diffusion layer

$$J = K_m \cdot (S - S_s) \quad (1)$$

2. Substrate mass transport inside the biofilm and microbial metabolism. Despite the fact that the biofilm internal structures are porous, consisting of microbial clusters separated by interstitial voids [5] and layered [6], in order to simplify the calculations, the assumption is made that the biofilm is continuous and that diffusion can be described by a single diffusion coefficient. Combining substrate utilisation with molecular diffusion throughout the biofilm a second-order differential equation is obtained. Using a Monod-type kinetic, the equation will be

$$\frac{\partial S_t}{\partial t} = D_f \frac{\partial^2 S_f}{\partial z^2} - \frac{k \cdot X \cdot S_f}{K_s + S_f} \quad (2)$$

Eq. (2) cannot be analytically integrated due to the nonlinearity of the Monod reaction term.

According to Wang *et al.* [7], for anaerobic expanded reactors working under low surface loads (below 3·5 mg chemical oxygen demand (COD) cm^{-2} d^{-1}), the thin biofilm can be assumed to be fully penetrated and internal diffusion resistance plays little or no role in the substrate utilization kinetics. On this condition, the Monod equation may be used to describe the anaerobic fluidized bed reactor (AFBR) performance

$$-\frac{dS_s}{dt} = \frac{k \cdot X \cdot S_s}{K_s + S_s} \quad (3)$$

Vertical segregation, so far neglected when modelling fluidized beds, was found to be significant in hydrodynamic behaviour [2,8]. It can be associated with the non-uniform biofilm growth on the support surface and can have an important effect on kinetic behaviour due to the differences in biomass concentration from the bottom to the upper part of the reactor.

The experiments carried out were designed in order to show the influence of initial acetate concentration, bed expansion, and bed segregation on the kinetic behaviour. Determination of the kinetic parameters was carried out by a computer program, PROGRESS (program for robust regression), that performs a robust regression based on the least median of squares and excludes outliers [9].

2. Materials and methods

2.1. Fluidized bed reactor

A scheme of the experimental installation is shown in Fig. 1. The fluidized bed reactor consists of a plexiglass column 19·3 cm in inner diameter and 200 cm tall. The reactor has six sampling ports uniformly located, and a recirculation pump in order to adjust the required bed expansion.

The carrier material employed was sepiolite. with 0·046 cm average diameter, and 1·44 g cm^{-3} average particle density. Sepiolite is a fibrous clay with a porous and rough surface that provides a shelter for bacteria from high fluid shear forces, improving microbial attachment. Sepiolite has been successfully used before as support media in different biofilm reactors [10,11].

The seed sludge, obtained from a mesophylic UASB (Upflow Anaerobic Sludge Blanket) reactor treating beet sugar wastewaters, was disintegrated before being, put into the experimental reactor. The AFBR was continuously fed for 18 months with the same synthetic wastewater, which implies that the hatch experiments were carried out with a mature biofilm. Organic loading rate remained with the range of 2·0–35 g COD $litre^{-1}$ d^{-1} and a hydraulic retention time between 5 and 18 h [2].

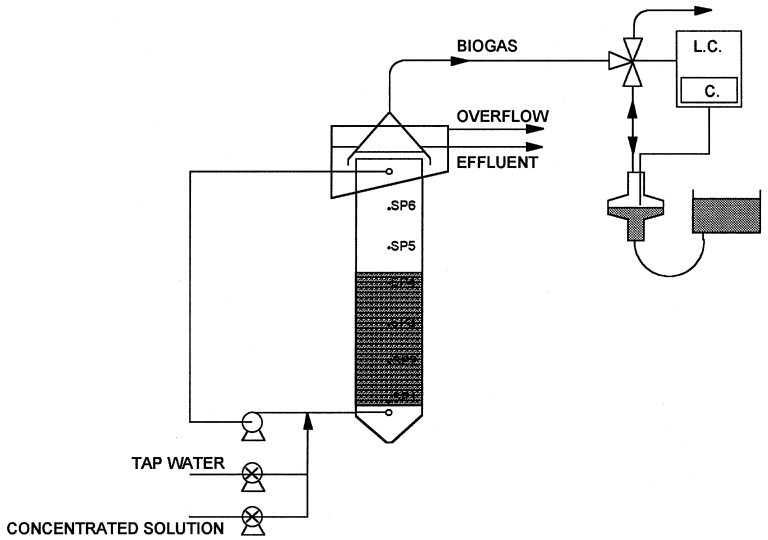

Fig. 1. Schematic diagram of the anaerobic fluidization bed. (SP, sampling ports; LC, level control; C, counter).

2.2. Synthetic wastewater

Synthetic wastewater was composed of acetic acid as the sole carbon source and a nutrient mixture, essential for maintaining an ideal environment for biological growth. The composition of the nutrient mixture is reported elsewhere [12]. The AFBR feeding was made by diluting a stock solution in tap water, to obtain the composition given in Table 1.

2.3. Experimental procedure

The determination of the substrate removal rate was carried out through a series of batch assays performed directly in the AFBR. Since a batch experiment was completed within a short period of time without alteration of microbial conditions in the reactor, the data obtained were representative of these conditions [13].

The assays were run with sludge loads ranging from 0·34 to 1·44 g HAc g VS^{-1}, adding to the reactor different amounts of stock solution neutralised with caustic soda. COD, biogas production and composition were determined every 15 min until biogas production stopped. During each assay, as acetic acid degradation advanced, hydrochloric acid was added to maintain the reactor pH between 7·1 and 7·3. All experiments were conducted in a temperature-controlled room maintained at 35 ± 1°C. The experimental conditions are listed in Table 2.

Runs from 1 to 6 were carried out with the whole bed, whereas runs 7 and 8 were carried out with different bed regions to study their particular behaviour. For run 7 the upper part of the bed, which from now on will be called C, was removed. In the same way, for run 8 the middle region, B, was also removed, with A being the remaining bed (Fig. 4).

The attached volatile solids were constant during all assays, which were performed consecutively. There was neither an increase nor a significant decrease associated with the growth, shearing or attrition processes.

2.4. Analyses

COD was analysed using the dichromate reflux method, and VS, based on settled volume of biocovered media, were measured according to Standard Methods for the Examination of Water and Wastewater [14]. As sepiolite itself showed some burning loss, in order to determine the attached biomass concentration, the obtained values of volatile solids were corrected by subtracting the contribution of the uncovered support.

The development of biofilm formation was followed by scanning electron microscopy (SEM). Differences in biomass distribution in samples from various reactor levels justified the differences in attached volatile solids concentration. Biogas production was measured with a wet-gas meter, and biogas composition was determined by gas chromatography (Hewlet Paekard 5170A), with a column packed with Porapak (Q 80/100) using thermal conductivity detection.

Table 1
Composition of synthetic influent wastewater

	Concentration (g $litre^{-1}$)
CH_3COOH	3·500
NH_4HCO_3	0·215
$NH_4H_2PO_4$	0·023
$MgSO_4 \cdot 7H_2O$	0·014
$CaCl_2$	0·001
NaOH	0·933

Table 2
Experimental conditions

Run number	S_0 (mg COD litre)	Expansion (%)	Region*
1	1430		
2	2870		
3	3820	37	A+B+C
4	5350		
5	2800	22	
6	2760	11	
7	1050		A+B
8	1810	37	A

* The bed was divided into three parts as shown in Fig. 4.

3. Results and discussion

3.1. Initial acetate concentration

Four assays using the same expansion but different initial acetate concentrations, between 1430 and 5350 mg COD litre^{-1}, were carried out (runs 1–4). Experimental results of these assays are presented in Fig. 2. The experimental points fit a straight line until the reactor organic matter depletes at which time the biogas production stops. Table 3 presents the slopes and its 95% confidence interval obtained by robust regression analysis of each run, once outliers were excluded.

In order to check that the rate of acetate degradation is independent from acetate concentration, results of the four runs were compared. The robust regression analysis of all the pairs (t, $S_{0i} - S$) did not discover new leverage points, which revealed that the four straight lines were parallel. The slope obtained this way was $K_0 = 1280 \pm 7$ mg COD litre^{-1} h^{-1}.

From these data, system evolution seems to be independent from acetate concentration. However at the beginning of the 4th assay, for the highest acetate concentration, COD removal and biogas production was slower. Experimental results of biogas production from third and fourth assays are shown in Fig. 3. These results can be due to methane-producing bacteria inhibition for an acetate concentration higher than 5000 mg COD litre^{-1}, which is certainly greater than the usual values during normal working conditions in mesophilic anaerobic reactors. After a short period of time in which the acetate removal rate was slower, the AFBR recuperated its normal activity.

During the linear period the substrate flux per unit of biofilm surface area can be calculated as a function of the support of the biocovered surface fraction, λ, using the equation

$$J = \frac{K_0 \cdot d_p}{6 \cdot \lambda \cdot (1 - \varepsilon_0)} \quad (4)$$

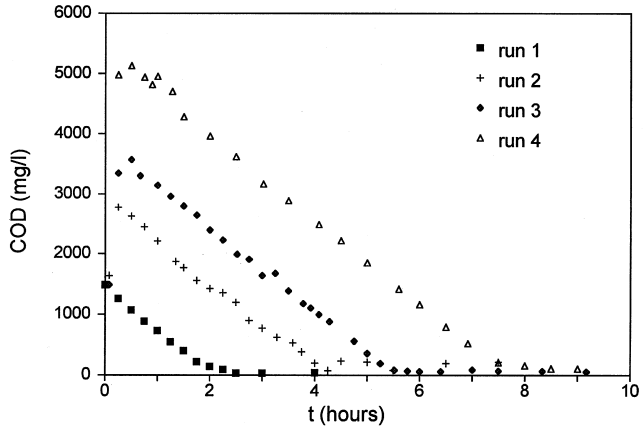

Fig. 2. COD concentration in the batches with different initial acetate concentrations.

It is difficult to determine accurately the biocovered surface fraction. With the aid of SEM, the bacteria on the sepiolite surface were found to be sparsely scattered in clumps, covering over half of the surface. Consequently, substrate flux per unit of biofilm surface area was below 0·78 mg COD cm^{-2} cm^{-1}, smaller than the critical value reported by Wang *et al.* [7] under which it can be assumed that diffusional resistance in the biofilm does not reduce the substrate concentration and Eq. (3) may be used. Finally, the linear decrease observed when the mixed liquor COD concentration > 100 mg litre^{-1} indicated that the saturation constant was smaller than this value, in accordance with the kinetic data from the literature for methane-producing bacteria, K, 30–100 mg litre^{-1} [15].

3.2. Bed expansion

Assuming that system evolution is independent of initial acetate concentration, two new assays were carried out, with different bed expansions, with the aim of knowing the influence of bed expansion on the kinetic behaviour, (runs 5 and 6). The experimental data were treated as aforementioned. Results are presented, together with the mean value of the previous four sets, in Table 4.

Mechanistically, it is difficult to explain that the COD removal rate was lower for 22% expansion than

Table 3
Initial acetate concentration effect[a]

Run number	S_0 (mg COD litre^{-1})	K_0^* (mg COD litre^{-1} h^{-1})
1	1430	1270 ± 96
2	2870	1260 ± 63
3	3820	1280 ± 30
4	5350	1300 ± 10

[a] Minimum fluidization volume basis.

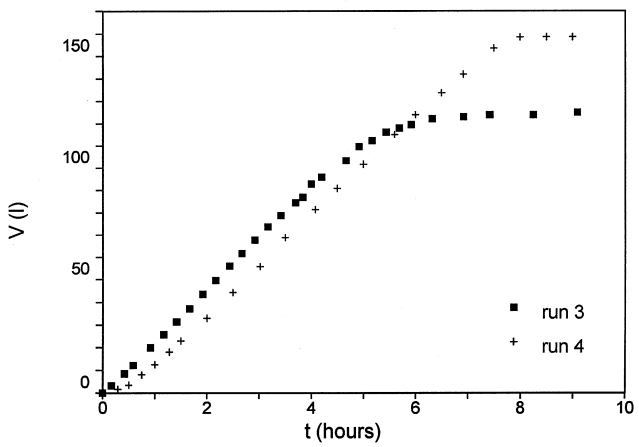

Fig. 3. Biogas volume versus time from the third and fourth assays.

for 37% expansion and in the same way lower than the one for 11% expansion. By means of the parallelism test described before it was checked that the difference in the K_0 values are not statistically significant. It can be assumed, therefore, that bed expansion had no effect on acetate kinetic removal.

In the studied expansion range, the value of the external soluble compounds transport coefficient, K_m, calculated by using semiempirical correlations [16,17], is between $5{\cdot}6 \times 10^{-5}$ and $7{\cdot}1 \times 10^{-5}$ m s^{-1}. By replacing these values in Eq. (1), it is possible to estimate that the difference $(S - S_s)$ is less than 1 mg COD-litre^{-1}. Therefore, external mass transport can be neglected, and then in Eq. (3), it is possible to replace S_s with S.

Assuming that the AFBR is a well-mixed system, Eq. (3) may be written

$$-\left(\frac{V}{V_0}\right)\cdot\frac{dS}{dt} = \frac{(k\cdot X\cdot V)}{V_0}\cdot\frac{S}{K_s + S} \quad (5)$$

The factor $k \cdot X \cdot V/V_0$ represents the maximum rate of substrate utilisation with regard to the bed volume at onset of fluidization, that before was presented as the slope of the linear period, K_0.

Table 4
Bed expansion effect

Run number	% Exp.	S_0 (mg COD litre^{-1})	K_0 (mg COD litre^{-1} h^{-1})
1–4	37%	1430–5350	1280 ± 7
5	22%	2800	1180 ± 40
6	11%	2760	1380 ± 40

Identifying VS with viable microbial population concentration, the maximum specific rate of substrate utilisation. k_s was calculated by dividing K_0, by the attached volatile solids concentration, 7·9 g VS litre^{-1}. The resulting k value was 162 ± 2 mg COD g VS^{-1} h^{-1}, in accordance with the kinetic data from the literature for methane-producing bacteria, $k = 100$–500 mg COD g VS^{-1} h^{-1} [18].

3.3. Bed segregation

With the aim of examining the influence of stratification on bed activity, two assays were conducted with different regions of the bed. The first one (run 7) was carried out after removing 29 cm of the top of the bed, and for the second one (run 8) 25 cm more was removed. It is therefore possible to distinguish three regions of the bed as presented in Fig. 4.

Table 5
Bed segregation effect

Run number	Region	S_0 (mg COD litre^{-1})	K_0 (mg COD litre^{-1} h^{-1})
1–6	A+B+C		1280 ± 14
7	A+B	1050	1120 ± 69
8	A	1810	990 ± 25

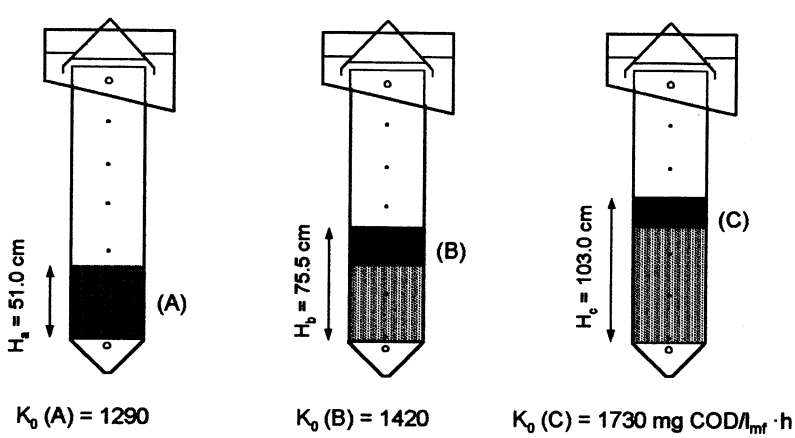

Fig. 4. Bed regions of segregation study.

Table 6
Activities of the different regions

Bed region	K_0 (mg COD litre^{-1} h^{-1})	VS (g VS litre^{-1})	k (mg COD g VS^{-1} h^{-1})
C	1720 ± 240	11·9	145 ± 20
B	1390 ± 260	7·5	185 ± 35
A	990 ± 5	5·0	198 ± 5

The experimental data were treated as in earlier experiments. Results (assays 7 and 8) are presented together with the mean value of assays 1 to 6, in Table 5. To check the bed segregation effect. it was verified that all the pairs $(t, S_0 - S)$ belonged to the same straight line. In this way, it was checked that the robust regression detected that the points of the last assays are outliers from the straight line that was formed by the pairs of the preceding assays. This means that the activity of the bottom part in the bed was different from (lower than) that in the bulk of the bed, expressed per bed volume.

The activity of each region was determined by subtracting the contribution of the lower levels

$$K_0(\mathrm{A}) = K_{0,8} \tag{6}$$

$$K_0(\mathrm{B}) = \frac{K_{0,7} \cdot H_\mathrm{B} - K_{0,8} \cdot H_\mathrm{A}}{H_\mathrm{B} - H_\mathrm{A}} \tag{7}$$

$$K_0(\mathrm{C}) = \frac{K_{0,1-6} \cdot H_\mathrm{C} - K_{0,7} \cdot H_\mathrm{B}}{H_\mathrm{C} - H_\mathrm{B}} \tag{8}$$

Results of the maximum rate in substrate utilisation with regard to the bed volume, K_0, VS concentration and maximum specific substrate utilisation rate, k, for the different regions are presented in Table 6. With regard to bed volume, the activity in the upper levels of the reactor (A, B) is greater than the activity in the bottom level (C). In contrast, with regard to the attached volatile solids concentration. the activity increases downwards. This is due to the fact the VS parameter, is extremely undefined as an index of active biomass. These results reveal that biomass concentration is lower downwards, where shear stress and attrition are important, but for the same reason in this area the fraction of active biomass on attached volatile solids is greater.

4. Conclusions

Kinetic data from an AFBR can be evaluated in batch experiments completed within a short period of time performed directly in the reactor. A zero-order acetate utilization pattern was consistently observed in all batch experiments until the reactor organic matter depleted anti biogas production stopped. The experiments showed that liquid film diffusion has no significant influence on the AFBR reaction rate.

At the maximum substrate removal rate, surface load is sufficiently low so that molecular diffusion within the biofilm can be neglected. Inhibition has been observed for acetate concentration higher than 5000 mg COD litre^{-1}. However, the phenomenon was not permanent, and the concentration decreased below the inhibitory value.

In the bottom level (C) where shear stress and attrition are the highest, the activity per volume unit, K_0, is lower than the activity of the upper levels (A, B). This means that the active biomass concentration is also lower in the bottom of the reactor. Nevertheless, the activity with regard to the attached volatile solids concentration, k, is higher in the bottom level than in the upper levels. This means that the active fraction of the attached volatile solids is greater in the region where shear stress and attrition are the highest.

Acknowledgements

The authors gratefully acknowledge support of this study by CICYT (Proyecto BIO92-0265-C02-01).

References

[1] Godia F, Sola C. Fluidized bed bioreactors (Review). Biotechnol Prog 1995;11(5):479–95.
[2] Diez V, Garcia PA, Fdz-Polanco F. Effects of biofilm growth, gas and liquid velocities on the expansion of an anaerobic fluidized bed reactor (AFBR). Wat Res 1995;29(7):1649–54.
[3] McCarty PL. Anaerobic waste treatment fundamentals: I. chemistry and microbiology. Public Works 1964;95(9):107.
[4] McCarty PL, Mosey FE. Modelling of anaerobic digestion processes (a discussion of concepts). Wat Sci Technol 1991;24(8):17–33.
[5] Lewandowski Z, Stoodley P, Altobelli S, Fukushima E. Hydrodynamics and kinetics in biofilm systems—recent advances and new problems. Wat Sci Technnol 1994;29(10–11):223–999.
[6] Imai. T, Kusoda T, Furumai H. Kinetic study and mathematical modeling of biofilm in an anaerobic fluidized bed. Wat Sci Technol 1994;29(10–11):369–76.
[7] Wang YT, Suidan MT, Rittmann BE. Modelling biofilm kinetic for low loaded expanded-bed reactor. J Environ Engng ASCE 1987;112:155–70.
[8] Csicor. Z, Mihaltz P, Czako L, Hollo J. A pressure test method monitors biofilm coated particle fluidization. Appl Microbiol Biotechnol 1995;43(2):363–86.
[9] Rousseeuw PJ. Tutorial to robust statistics. J Chemom 1991;5:1–20.

[10] Borja R, Banks CJ, Maestrojuan GM, Wang Z. Antgonistic and synergistic effects of two mineral support particles on the hydrolysis anti methanation of waste water in immobilized cell anaerobic digesters. Biotechnol Lett 1994;16(8):859–64.
[11] Iza J, Garcia PA, Sanz I, Hernando S, Fdz-Polanco F. Anaerobic fluidized bed reactors (AFBR): performance and hydraulic behaviour. In: Hall, Hobson, editors. Advances in Water Pollution control. Anaerobic Digestion. New York: Pergamon, 1988:155–63.
[12] Hulshoff Pol LW, de Zceuw WJ, Velzeboer CTM, Lettinga G. Granulation in UASB-reactor. Wat Sci Technol 1983;15:291–304.
[13] Nguyen VT, Shieh WK. Evaluation of intrinsic and inhibition kinetics in biological fluidized bed reactors. Wat Res 1995;29(11):2520–4.
[14] American Public Health Association. Standard Methods for the Examination of Water and Wastewater, 17th. Washington, DC: APHA, 1989.
[15] Henze M, Harremoës P, Hansen JC, Arvin E. Waste Water Treatment. Biological and Chemical Processes. Berlin: Springer, 1995.
[16] Wilson E, Geankoplis C. Liquid mass transfer at very low numbers in paeked beds. Ind Engng Chem Fundam 1966;59:00–0.
[17] Shich WK, Keenan JD. Fluidized bed biofilm reactor for wastewater treatment. Adv Biochem Engng Biotechnol 1986;33:132–69.
[18] Henze M, Harremoës P. Anaerobic treatment of wastewaters in fixed film reactors. A literature review. Wat Sci Technol 1994;15:1–101.